

# Effect of the input base rocking on the relative response of long buildings on embedded foundations

M.I. Todorovska\*, M.D. Trifunac\*\*

**ABSTRACT** – A two dimensional building-foundation-soil interaction model has been used to study how much the lateral forces in long buildings may be underestimated by neglecting the input rocking excitation, and by approximating the foundation input motion in soil-structure interaction problems by a frequency independent translation only. The ratio  $\mathcal{R}(\eta) = |u_b^{\text{rel}}|/|u_{b,\text{com}}^{\text{rel}}|$  has been studied, where  $u_b^{\text{rel}}$  is the response at dimensionless frequency  $\eta$  to the «true» foundation input motion, and  $u_{b,\text{com}}^{\text{rel}}$  is the response to the «common» approximation (horizontal motion only) of the foundation input motion. Three «buildings» have been analyzed: 1, 10, and 50-storeys high, represented by equivalent single degree-of-freedom oscillators, supported by circular foundations (depth-to-half-width ratio  $h/a = 1$  and  $0.5$ ) embedded in a homogeneous and elastic half-space, and excited by plane P- and SV-waves and by surface Rayleigh-waves.

The results show that  $\mathcal{R}(\eta)$  is mostly affected by the amplitude of the rocking component of the foundation input motion,  $\phi^{\text{inp}}$ , and by the building height.  $\mathcal{R}(\eta)$  is larger when the input rotation is larger and when the building is higher. Of all the excitations considered, the foundation input rotation is the largest for incident SV-waves beyond critical angle and for incident Rayleigh-waves. For the cases studied, for incident Rayleigh-waves and for semi-circular foundation,  $\mathcal{R}(\eta)$  can be as large as 3 for the 1-storey building, 5 for the 10-storey building, and 9 for the 50-storey building. For higher buildings, the building and the foundation masses affect  $\mathcal{R}(\eta)$  through the compliance forces that modify the displacement at the building base. For a 50-storey building model,  $\mathcal{R}(\eta)$  is smaller when the building and the foundation masses are larger. Because of 1/ the simplicity of the soil representation and 2/ the two dimensional nature of the building models, the results in this paper can be considered only to apply for transverse vibrations of long buildings responding mainly in the first mode of vibration. More detailed quantitative studies must include detailed modeling of the geology at the building site, three-dimensional building and foundation models, and use of recorded rock-

ing accelerograms (when those become available). We leave analyses of these model characteristics for a future paper.

## Introduction

In the common engineering practice, the rocking component of the input motion of buildings exposed to strong earthquake ground shaking is usually neglected. Even in analyses that include the soil-structure interaction effects, the lateral forces in the building components are evaluated assuming only horizontal foundation input motion (the foundation input motion is approximated by horizontal translation with constant amplitude for all frequencies). This corresponds typically to vertically incident shear waves and buildings on surface foundations. The rotational components of the input motion are included usually only in specialized analyses using soil-structure interaction models (Luco, 1980). The aim of this paper is to begin with some simple estimates of how much larger the forces in the buildings may be if the input rocking is not neglected.

Studies have shown (Trifunac, 1982; Todorovska and Trifunac, 1990) that the rocking component of ground motion may not be negligible in contributing to the total base excitation of buildings (e.g. plane SV-waves in a half-space with incidence beyond critical angle, and incident surface Rayleigh-waves). For buildings on softer soils and on embedded foundations, the input base rocking can be significant even when the free-field motion has zero point rotation (e.g. vertically incident SV-waves in a half-space or plane SV-waves in a half-space with incidence at critical angle). In a more realistic geologic environment, such as layered half-space, it has been shown (Trifunac, 1971, 1972) that as much as 70 to 90 percent of the energy arriving at a site, from distant or shallow earthquakes, may be via surface waves. Lomnitz (1990) considers the exist-

\* Research Assistant Professor

\*\* Professor, Civil Eng., University of Southern California, Los Angeles, CA 90089-2531

ence of surface gravity waves in the soft sediments of Mexico City during the 1985 earthquake, locally generated after a transition from elastic to hydrodynamic regimes at a critical strain level. Those waves would have wave lengths  $\sim 20$  m, decay very fast with depth, would be characterized by a prograde elliptical particle motion, and would produce large strains and rocking close to the surface. Lomnitz discusses the possibility that those short surface waves might have been responsible for the damage of many modern high-rise buildings with shallow foundations, while harming only little the old colonial buildings that, over the years, had sunk at least two stories below street level, due to their weight.

Because of lack of recordings of rotational components of strong ground motion, attempts have been made to construct rocking and torsional accelerograms from the recorded translational components of the ground motion (Lee and Trifunac, 1985, 1987; Castellani and Boffi, 1986, 1989; Niazi, 1986). For example, the computer code NSYNACC (Lee and Trifunac, 1985, 1987) generates rocking and torsional free-field time histories at a point on the surface, given the geologic structure (approximated by horizontal layers) and the Fourier spectra of recorded translational components of motion at the site. Niazi (1986) used conventional recordings of the 1979 Imperial Valley, California earthquake by the El Centro Differential Array to estimate the rocking and torsional components of strong ground motion. Gupta and Trifunac (1990a,b) included rocking excitation in the analysis of the response of buildings by probabilistic spectrum superposition methods. In Gupta and Trifunac (1990a), the amplitude and phase of the input rocking were those for a homogeneous half-space with plane-wave incidence, and in Gupta and Trifunac (1990b), those calculated by NSYNACC. Further studies have shown that tall buildings, supported by soft soil (shear wave velocity less than 100 m/sec) and excited by distant large earthquakes (with prominent spectral peaks in the long period range,  $T > 1$  sec), can experience larger shear forces and bending moments than what is indicated by the conventional analyses. It has been shown (Gupta and Trifunac 1989; 1991) that these increases can be attributed to the additional excitation by ground rocking. However, these studies did not address the kinematic soil-structure interaction, to see which aspects of the wave passage effects play the prominent role in this process. Thus, one aim of the present work is to initiate analyses of those additional effects, first under simple and controlled conditions, enabling us to outline the most likely conditions where the wave passage effects play an important role in contributing to larger shear forces and overturning moments in response of buildings to strong earthquake excitation.

The study in this paper is a continuation of the work of Todorovska and Trifunac (1990, 1992). The amplification of the relative building response, due to the input base rocking excitation, is analyzed using the same two dimensional (2D) model as in Todorovska and Trifunac (1992), for incident plane P- and SV-waves and surface Rayleigh-waves. In this model, the

soil is represented by a homogeneous elastic half-space and the building is an equivalent single degree-of-freedom oscillator supported by a circular rigid embedded foundation. The real buildings are three-dimensional, they usually have prismatic foundations, for taller buildings the contribution of the higher modes of vibration to the response should not be neglected, and a homogeneous elastic half-space and plane incident waves are too crude idealizations of the realistic geology under the building site and of a realistic earthquake excitation. Thus, the purpose of this paper is only to illustrate how large the contribution of the rocking component of the foundation input motion could be, for simple two-dimensional models, and to see for which parameters of the building soil system such contributions may be important.

### The model

The model (Fig. 1) is an equivalent single degree-of-freedom oscillator (mass  $m_b$  per unit length in the  $y$ -direction, height  $H$ , radius of gyration  $r_b$ , fixed-base natural frequency  $\omega_N$  and damping ratio  $\zeta$ ) on a rigid circular foundation (width  $2a$ , depth  $h$ , and mass  $m_f$  per unit length in the  $y$ -direction), embedded in a homogeneous half-space (shear wave velocity,  $\beta$ , shear modulus,  $\mu$  and Poisson's ratio  $\nu$ ). The oscillator consists of a bar with concentrated mass at one end, and a rocking spring with a dashpot at the other end, connecting it to the foundation at point O. The center of the foundation surface is at O, and the model response, relative to the foundation, is measured by the angle  $\psi^{rel}$ . The foundation motion is described by the horizontal translation  $\Delta$  (positive to the right) and the vertical translation  $V$  (positive down) from point O, and by the clockwise rotation  $\varphi$  about O. Using a linear analysis, the relative response of the oscillator, in terms of monochromatic motion at the base  $\Delta = \Delta_0 e^{-i\omega t}$  and  $\varphi = \varphi_0 e^{-i\omega t}$ , is  $\psi^{rel} = \psi_0^{rel} e^{-i\omega t}$  where

$$\psi_0^{rel} = \frac{\frac{m_b H^2}{I_0} \left( \frac{\omega}{\omega_N} \right)^2 \frac{\Delta_0}{H} + \left[ \left( \frac{\omega}{\omega_N} \right)^2 + \frac{g}{\omega_N^2 H} \frac{m_b H^2}{I_0} \right] \varphi_0}{1 - 2i\zeta \frac{\omega}{\omega_N} - \left( \frac{\omega}{\omega_N} \right)^2 - \frac{g}{\omega_N^2 H} \frac{m_b H^2}{I_0}} \quad (1)$$

In Eq. (1),  $g$  is the acceleration due to gravity, and

$$I_0 = m_b H^2 \left[ 1 + \left( \frac{r_b}{H} \right)^2 \right]$$

is the moment of inertia of the oscillator about O. The height,  $H$ , and the radius of gyration,  $r_b$ , of the equivalent oscillator can be related to the height,  $H_{sb}$ , and width,  $W_{sb}$ , of a homogeneous shear beam building model, with same mass above foundation level and same moment of inertia about

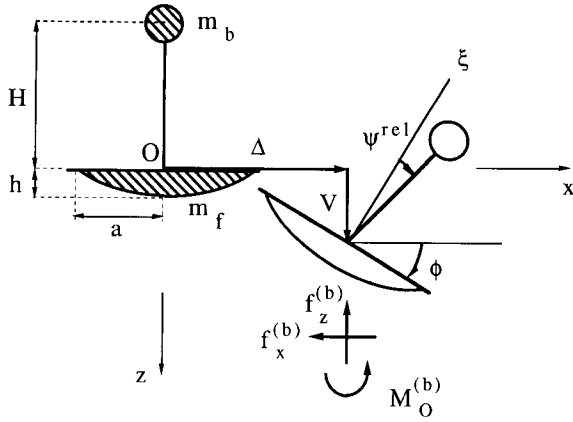


Fig. 1 – The model: an equivalent single degree-of-freedom oscillator, supported by a circular foundation embedded into a homogeneous elastic half-space, and excited by incident plane P- and SV-waves, or by surface Rayleigh waves. The oscillator consists of a rod with a concentrated mass at one end, and a rocking spring and a dashpot (not shown in this figure) at the other end.  $\Delta$ ,  $V$  and  $\phi$  are the absolute horizontal, vertical translations, and the rotation of the foundation about point  $O$ .

point  $O$  on the base, as:  $H = H_{sb} / \sqrt{3}$  and  $r_b = W_{sb} / \sqrt{12}$ . The terms in Eq. (1) that include  $g$  come from the dynamic moment of the gravity forces acting on the oscillator. Those are neglected in the calculations in this paper.

The equations of motion of the system result from the dynamic equilibrium equations of the foundation. For monochromatic excitation, with circular frequency  $\omega$ , those can be written in matrix form as:

$$[M_f]\Delta = \mathbf{F}^{(b)} - \mathbf{F}^{(s)} - \mathbf{F}_g^{(f)} \quad (2)$$

where  $[M_f] = \text{diag}\{m_f, m_f, I_0^{(f)} / H^2\}$  is the mass matrix of the foundation, and  $\Delta = \{V, \Delta, \phi H\}^T$  is the generalized displacement vector of the foundation.  $\mathbf{F}^{(b)} = \{f_z^{(b)}, f_x^{(b)}, M_0^{(b)} / H\}^T$ ,  $\mathbf{F}^{(s)} = \{f_z^{(s)}, f_x^{(s)}, M_0^{(s)} / H\}^T$  and  $\mathbf{F}_g^{(f)} = \{0, 0, m_f g c \phi / H\}^T$  are generalized force vectors of the outside vertical and horizontal forces and moments (about  $O$ ) acting on the foundation.  $f_z^{(b)}$  (pointing down),  $f_x^{(b)}$  (pointing to the right) and  $M_0^{(b)}$  (clockwise) are exerted by the building;  $f_z^{(s)}$  (pointing up),  $f_x^{(s)}$  (pointing to the left) and  $M_0^{(s)}$  (counter-clockwise) are exerted by the soil;  $m_f g c \phi$  (counter-clockwise) is the moment of the gravity forces acting on the foundation and  $c$  is the coordinate of the center of gravity of the foundation. The moments of the vertical inertia forces of the building and of the foundation have been neglected both in Eq. (1) and in Eq. (2), because they produce second order terms of the foundation and relative building displacements (the analysis in this paper is linear).

Expressions for  $\mathbf{F}^{(b)}$  can be found in Appendix B. It is customary to decompose  $\mathbf{F}^{(s)}$  into two vectors  $\mathbf{F}_0^{(s)}$  and  $\mathbf{F}_\Delta^{(s)}$ .  $\mathbf{F}_0^{(s)}$  represents the foundation driving forces, which represent the integrals of the stresses produced by the free-field motion and acting on the foundation

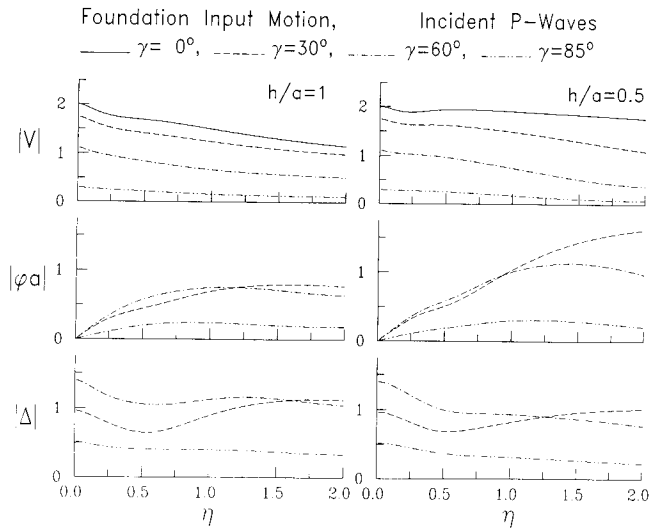


Fig. 2 – Foundation input motion (response of a massless rigid foundation to the incident waves), versus the dimensionless frequency  $\eta$ , for a semi-circular ( $h/a = 1$ ) and for a shallow ( $h/a = 0.5$ ) foundation. The excitation is a plane P-wave with unit displacement amplitude.

kept at rest. Those are equal in magnitude and act in opposite direction of the forces that must be applied to the foundation to keep it at rest when it is exposed to the action of the free-field motion. The components of  $\mathbf{F}_\Delta^{(s)}$  are integrals of the stresses induced in the half-space, as it deforms because of the moving foundation.

$$\mathbf{F}_\Delta^{(s)} = -2\mu[Q]\Delta, \quad (3)$$

and  $2\mu[Q]$  is the foundation impedance matrix.  $\mathbf{F}_\Delta^{(s)}$  is equal in magnitude, but with opposite sign of the generalized force vector of the outside forces that must be applied to the (massless) foundation to displace it by generalized displacement vector  $\Delta$ .

The displacement of a massless foundation under the action of the incident waves, in the absence of any other external forces, is usually called foundation input motion and in this paper it will be denoted by  $\Delta^{\text{inp}} = \{V^{\text{inp}}, \Delta^{\text{inp}}, \phi^{\text{inp}} H\}^T$ . Then the foundation driving forces  $\mathbf{F}_0^{(s)}$  can be expressed in terms of  $\Delta^{\text{inp}}$  and of the foundation impedance matrix  $[Q]$

$$\mathbf{F}_0^{(s)} = 2\mu[Q]\Delta^{\text{inp}}. \quad (4)$$

Analytical expression for  $[Q]$  and for  $\mathbf{F}_0^{(s)}$  (for incident plane P- and SV-waves and incident Rayleigh waves) for cylindrical foundations can be found in Todorovska and Trifunac (1990).

## Results and analysis

### FOUNDATION INPUT MOTION

For building models on rigid foundations, the foundation input motion is the response of the foundation, assumed to be massless, in the absence of the building. In general, the foundation input motion differs from the

free-field motion on the half-space surface. (The free-field motion is the motion of the half-space in the absence of any irregularities.) In Fig. 2, Fig. 3, and Fig. 4, the foundation input motion is shown versus the dimensionless frequency  $\eta$  ( $\eta = 2a/\beta T$ , where  $T$  is the period of the excitation) for incident plane P-waves (Fig. 2), plane SV-waves (Fig. 3), with unit displacement amplitude, and surface Rayleighwaves (Fig. 4), with unit horizontal displacement amplitude on the half-space surface. The incident P-waves have angles of incidence (measured from the vertical)  $\gamma = 0^\circ, 30^\circ, 60^\circ$  and  $85^\circ$  and the SV-waves have angles of incidence  $\gamma = 0^\circ, 30^\circ, 45^\circ, 60^\circ$  and  $85^\circ$ . For incident P-waves and SV-waves below critical angle (Poissons ratio  $\nu = 0.3333$  in all the examples, implying  $\gamma_{\text{crit}} = 30^\circ$ ), the foundation input motion is shown for a semicircular foundation ( $h/a = 1$ ) and for a shallow foundation ( $h/a = 0.5$ ). For incident SV-waves beyond critical angle and for Rayleigh-waves, curves are shown only for  $h/a = 1$ , because of the insufficient accuracy of the numerical calculations for smaller values of  $h/a$ . A further and a more detailed interpretation of the characteristics of the foundation input motion as in Fig. 2, Fig. 3, and Fig. 4 can be found in Todorovska and Trifunac (1990).

In calculations of the lateral forces in buildings, the dependance of  $\Delta^{\text{inp}}$  on the wavelength of the incident waves is usually neglected, and  $\varphi^{\text{inp}}$  is assumed to be equal to zero. The common approximation of the foundation input motion,  $\Delta_{\text{com}}^{\text{inp}}$ , consists only of a translation, with amplitude equal to the horizontal amplitude of the free-field motion on the surface,  $u^{\text{ff}}$ . In Figs. 2, 3, and 4,  $u^{\text{ff}}$  is the limit of  $\Delta^{\text{inp}}$  as  $\eta \rightarrow 0$ . Taking the relative horizontal response  $u_b^{\text{rel}} = \psi^{\text{rel}} H$  to be representative of the lateral forces in the buildings, in this paper, the relative response  $u_b^{\text{rel}}$ , produced by incident waves with foundation input motion as in Fig. 2, Fig. 3, and Fig. 4 will be compared with the relative response  $u_{b,\text{com}}^{\text{rel}}$  produced by foundation input motion  $\Delta_{\text{com}}^{\text{inp}} = \{0, u^{\text{ff}}, 0\}^T$ . Comparing  $\Delta^{\text{inp}}$  in Fig. 2 and Fig. 3 with  $\Delta_{\text{com}}^{\text{inp}}$  it can be seen that  $\Delta_{\text{com}}^{\text{inp}}$  overestimates the horizontal displacement at higher frequencies, but ignores the rotation at all frequencies. As  $\eta \rightarrow 0$  (i.e. the wavelength of the incident waves is very long),  $\Delta^{\text{inp}} \rightarrow \Delta_{\text{com}}^{\text{inp}}$  and  $\varphi^{\text{inp}} \rightarrow 0$ . However, for incident SV-waves beyond critical angle and for incident Rayleigh-waves, the rotation  $\varphi^{\text{inp}}$  is not negligible even for relatively small values of  $\eta$ . How this will affect the response of buildings of different height, will be illustrated by the following examples.

#### EXAMPLE BUILDINGS

Three example «buildings» will be considered: /1/ a single storey building (height 5 m, width 10 m and fixed-base natural frequency  $T_N = 0.1$  sec), /2/ a 10 storey building (height 50 m, width 20 m and fundamental fixed-base frequency  $T_N = 1$  sec), and /3/ a 50 storey building (height 250 m, width 30 m and fundamental fixed-base frequency  $T_N = 5$  sec). It is assumed that the width of the building is equal to the width of the foun-

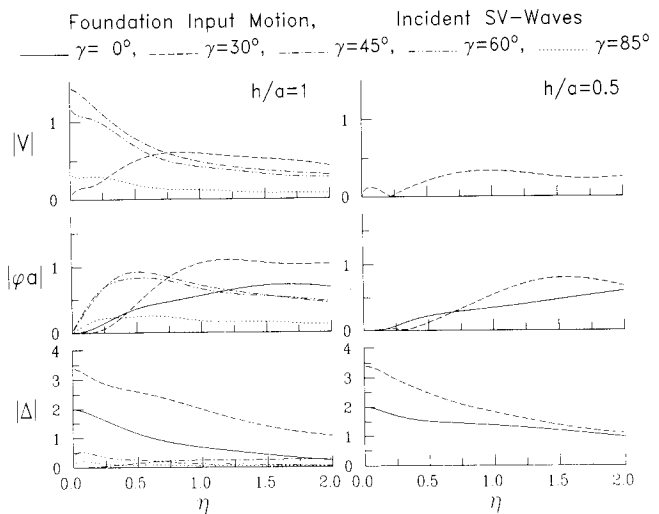


Fig. 3 – Foundation input motion (response of a massless rigid foundation to the incident waves), versus the dimensionless frequency  $\eta$ , for a semi-circular ( $h/a = 1$ ) and for a shallow ( $h/a = 0.5$ ) foundation. The excitation is a plane SV-wave with unit displacement amplitude.

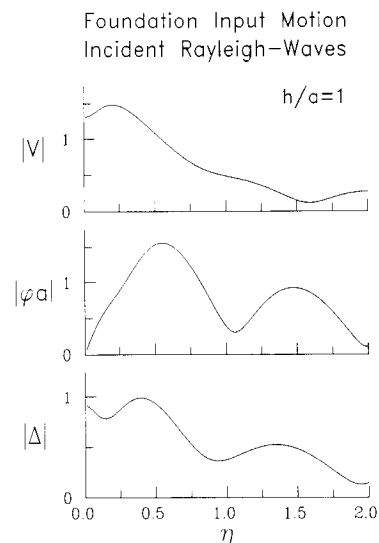


Fig. 4 – Foundation input motion (response of a massless rigid foundation to the incident waves), versus the dimensionless frequency  $\eta$ , for a semi-circular foundation ( $h/a = 1$ ). The excitation is a surface Rayleigh-wave with unit horizontal displacement amplitude.

dation,  $2a$ , and that, typically, the ratio between the density of the building and of the soil  $\rho_b/\rho_s \approx 0.2$ . The properties of the equivalent shear beam models (Todorovska and Trifunac, 1990) and of the equivalent single degree-of-freedom models that correspond to those three «buildings» are given in Table 1. (Both models have same mass and same moment of inertia about point  $O$ , which implies  $H = H_{\text{sb}}/\sqrt{3}$  and  $r_b = W_{\text{sb}}/\sqrt{12}$ .) Also, in this table, the dimensionless fixed-base fre-

quency  $\eta_N = \frac{2a}{\beta T_N}$  is given for two values of the shear-

wave velocity in the soil:  $\beta = 1000$  m/s («hard» soil) and  $\beta = 50$  m/s («soft» soil, e.g. in Mexico City). The ratio  $m_b/m_s$  is for a semi-circular foundation.  $n$  denotes the number of stories. Guided by the values in Table 1, the following values of  $H/a$ ,  $m_b/m_t$  and  $m_t/m_s$  will be

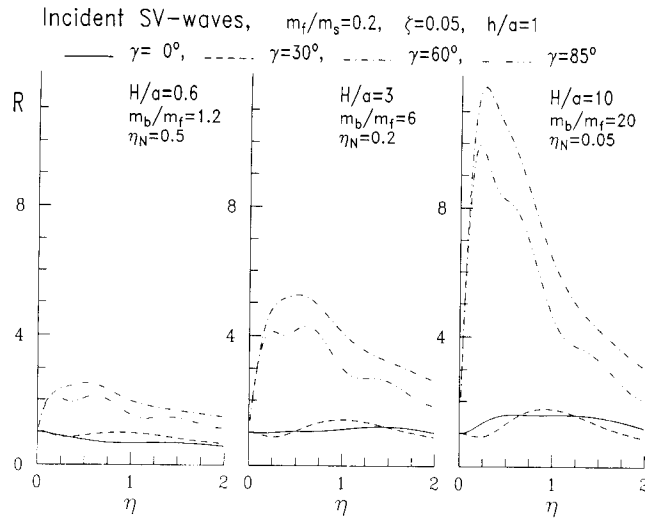


Fig. 5 –  $R \equiv \mathcal{R}$  (the ratio of the relative response to the «true» foundation input motion  $\Delta^{\text{inp}}$  and to the «common» approximation  $\Delta^{\text{com}}$ ), versus the dimensionless frequency  $\eta$ , for incident plane SV-waves, for three buildings (a 1-storey, a 10-storey, and a 50-storey) on semi-circular foundations. The different lines correspond to different incident angles.

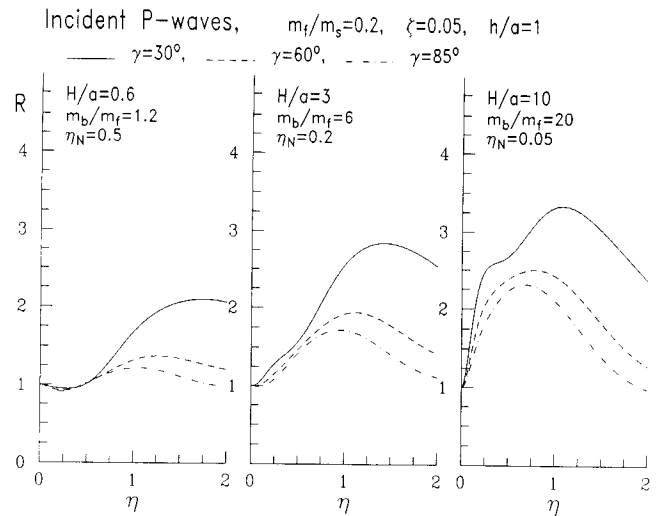


Fig. 6 –  $R \equiv \mathcal{R}$  (the ratio of the relative response to the «true» foundation input motion  $\Delta^{\text{inp}}$  and to the «common» approximation  $\Delta^{\text{com}}$ ), versus the dimensionless frequency  $\eta$ , for incident plane P-waves, for three buildings (a 1-storey, a 10-storey, and a 50-storey) on semi-circular foundations. The different lines correspond to different incident angles.

used in the calculations:

$$\begin{array}{lll} n=1 & H/a=0.6 & \frac{m_b}{m_f}=0.3, 0.6, 1.2 \quad \frac{m_f}{m_s}=0.2 \\ n=10 & H/a=3 & \frac{m_b}{m_f}=1.5, 3, 6 \quad \frac{m_f}{m_s}=0.2 \\ n=50 & H/a=10 & \frac{m_b}{m_f}=5, 10, 20 \quad \frac{m_f}{m_s}=0.2 \end{array}$$

In some of the examples, a range of values of  $m_b/m_f$  is taken for each value of  $H/a$ ; the second value of  $m_b/m_f$  corresponds to the typical value  $\rho_b/\rho_s \approx 0.2$ ; the first and the third values of  $m_b/m_f$  correspond to twice and half of the typical value of  $\rho_b/\rho_s$ .

#### THE SYSTEM RESPONSE

The soil-structure system (Fig. 1) responds with translation and rocking of the foundation, and by motion of the oscillator relative to the foundation. The transfer-function between the oscillator relative response and the incident wave motion differs from the transfer-function of a fixed-base model. The frequency and the amplitude of the peak in the transfer-function of a flexible-base building depend on the shear-wave velocity and the damping in the soil, on the building mass, height and fixed-base frequency, and on the foundation mass and shape. The system frequency (the frequency of the peak) is always smaller than the fixed-base frequency; the lower limit is the system frequency of a rigid building oscillating in the elastic half-space. In this paper,  $\eta^{\text{sys}}$  is the dimensionless system frequency (it is the frequency of the peak response, when the

transfer-function is in terms of the dimensionless frequency  $\eta$ ). The amplitude of the peak in the relative response transfer function is always smaller for this model than for the fixed-base model (Todorovska and Trifunac, 1992). This is, however, not always the case if there is material damping in the soil (Bielak, 1971). In the limit when the soil is infinitely stiff compared with the building, the system frequency approaches the fixed base frequency, and the peak relative response approaches the fixed base peak relative response.

#### AMPLIFICATION OF THE RELATIVE RESPONSE

To see how much larger the relative response may be because of the presence of the rocking input motion, the ratio  $\mathcal{R}(\eta) = |u_b^{\text{rel}}|/|u_{b,\text{com}}^{\text{rel}}|$ , where  $u_b^{\text{rel}}$  is the response to the «true» excitation and  $u_{b,\text{com}}^{\text{rel}}$  is the response to the «common» excitation, was calculated for the three example buildings. The «true» excitation is the foundation input motion for incident plane P- and SV-waves and Raleigh waves, normalized by the amplitude of the horizontal component of the free-field motion (Fig. 2 and Fig. 3). The gravity forces are neglected in all the calculations of  $u_b^{\text{rel}}$ . From Eq. (1), neglecting the terms involving  $g$  it follows

$$u_b^{\text{rel}} = \psi H = C(\omega, \omega_N, \zeta) \left[ \frac{1}{1 + \left(\frac{r_b}{H}\right)^2} \Delta + \varphi H \right] \quad (5)$$

where  $C(\omega, \omega_N, \zeta)$  is a function describing the response characteristics of the fixed base building model, and  $\Delta$

and  $\varphi$  are the horizontal and the rocking motions of the building base. Then

$$\mathcal{R}(\eta) = \frac{|C(\omega, \omega_N, \zeta) \left[ \frac{1}{1 + \left(\frac{r_b}{H}\right)^2} \Delta + \varphi H \right]|}{|C(\eta, \eta_N, \zeta) \left[ \frac{1}{1 + \left(\frac{r_b}{H}\right)^2} \Delta_{\text{com}} + \varphi_{\text{com}} H \right]|} \quad (6)$$

$$\leq \frac{|C(\eta, \eta_N, \zeta) \left[ \frac{1}{1 + \left(\frac{r_b}{H}\right)^2} \Delta + \varphi H \right]|}{|C(\eta, \eta_N, \zeta) \left[ \frac{1}{1 + \left(\frac{r_b}{H}\right)^2} \Delta_{\text{com}} + \varphi_{\text{com}} H \right]|}$$

which implies

$$\mathcal{R}(\eta) \leq \frac{\left| \frac{1}{1 + \left(\frac{r_b}{H}\right)^2} \Delta + \varphi H \right|}{\left| \frac{1}{1 + \left(\frac{r_b}{H}\right)^2} \Delta_{\text{com}} + \varphi_{\text{com}} H \right|} \quad (7)$$

In Eq. (7),  $\Delta$  is a sum of  $\Delta^{\text{inp}}$  and the translation relative to  $\Delta^{\text{inp}}$  due to the compliance forces;  $\varphi$  is a sum of  $\varphi^{\text{inp}}$  and of the rotation due to the compliance forces. Similarly,  $\Delta_{\text{com}}$  is a sum of  $\Delta_{\text{com}}^{\text{inp}} (= u^{\text{ff}})$  and the translation due to the compliance forces, but  $\varphi_{\text{com}}$  is equal only to the rotation due to the compliance forces. These additional displacements due to the dynamic forces from the building depend on the building mass and height, on the foundation mass, and on the flexibility of the soil relative to the building.  $\varphi^{\text{inp}}$ , as a part of  $\varphi$  in the numerator of Eq. (6), multiplies  $H$ , which implies that  $\mathcal{R}(\eta)$  is larger when the building is higher.

The results for the example buildings show that  $\mathcal{R}(\eta)$  depends mostly on  $H/a$  and on  $\varphi^{\text{inp}}$  ( $\mathcal{R}(\eta)$  is larger when

Incident Rayleigh-waves,  $m_b/m_s=0.2$ ,  $\zeta=0.05$ ,  $h/a=1$

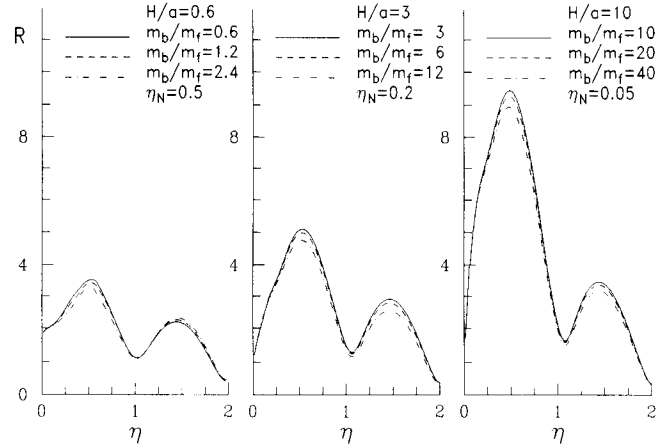


Fig. 7 –  $R \equiv \mathcal{R}$  (the ratio of the relative response to the «true» foundation input motion  $\Delta^{\text{inp}}$ , and to the «common» approximation  $\Delta_{\text{com}}^{\text{inp}}$ ), versus the dimensionless frequency  $\eta$ , for incident surface Rayleigh-waves, for three buildings (a 1-storey, a 10-storey, and a 50-storey) on semi-circular foundations. The different lines correspond to different values of the building mass.

$H/a$  is larger and when  $\varphi^{\text{inp}}$  is larger), but also on  $m_b/m_s$  and  $m_b/m_t$ . (The building and foundation masses affect  $\mathcal{R}(\eta)$  through the «compliance» displacements and rotations, as part of  $\Delta$ ,  $\varphi$ ,  $\Delta_{\text{com}}$  and  $\varphi_{\text{com}}$ ).  $\mathcal{R}(\eta)$  does not depend much on the resonance characteristics of the building, i.e. on  $\omega/\omega_N$  and  $\zeta$ . Therefore, in Eq. (7), the « $\leq$ » sign can be substituted with « $\approx$ ».

The dependance of  $\mathcal{R}(\eta)$  on  $\varphi^{\text{inp}}$  (type of incident waves and their angle of incidence) and on  $H/a$  is illustrated in Fig. 5, Fig. 6, and Fig. 7, where the excitation consists of plane SV-waves, plane P-waves and Rayleigh-waves, respectively. The plots on the left-hand-side of these figures are for a 1-storey building ( $H/a = 0.6$ ,  $m_b/m_t = 1.2$ , and  $\eta_N = 0.5$ ); the plots in the middle are for a 10-storey building ( $H/a = 3$ ,  $m_b/m_t = 6$ , and  $\eta_N = 0.2$ ); the plots on the right-hand-side are for a 50-storey building ( $H/a = 10$ ,  $m_b/m_t = 20$ , and  $\eta_N = 0.05$ ). The foundation is semi-circular ( $h/a = 1$ ),  $m_b/m_s = 0.2$ , and  $\zeta = 0.05$  in all the three figures. The different lines in Fig. 5 and Fig. 6 correspond to different incident angles, and in Fig. 7 to different values of the building mass. It can be seen from these three figures that the amplification  $\mathcal{R}(\eta)$  increases with the height of the building, and that it is proportional to the amplitude of the rotation of the foundation input motion,  $\varphi^{\text{inp}}(\eta)$ . Since  $\mathcal{R}(\eta)$  depends very little on the value of  $\eta_N$ , the results in these figures can be used to estimate  $\mathcal{R}(\eta)$  for any value of  $\eta_N$ .

#### Incident SV-waves

From Fig. 3, it can be seen that  $\varphi^{\text{inp}}$  is larger for  $\gamma = 60^\circ$  and  $85^\circ$  than for  $\gamma = 0^\circ$  and  $30^\circ$ . The shapes of the curves  $\mathcal{R}(\eta)$  are also different. For  $\gamma = 60^\circ$  and  $85^\circ$ ,  $\varphi^{\text{inp}}(\eta)$  grows faster with  $\eta$  and is the largest for  $\eta \approx 0.5$ ; for  $\gamma = 0^\circ$  and  $30^\circ$ ,  $\varphi^{\text{inp}}$  is small for lower  $\eta$ 's and is larger only for  $\eta > 1$ . On the other hand,  $\Delta^{\text{inp}}$  decays

as  $\eta$  increases, and for  $n > 1$  and for  $\gamma = 0^\circ$  and  $30^\circ$  it has decreased almost to half of the value of  $\Delta_{\text{com}}^{\text{inp}}$  (Fig. 3). This is reflected in the shape and in the amplitude of  $\mathcal{R}(\eta)$  (Fig. 5), which is considerably larger for  $\gamma = 60^\circ$  and  $85^\circ$  than for  $\gamma = 0^\circ$  and  $30^\circ$ . For  $\gamma = 60^\circ$  and  $85^\circ$ ,  $\mathcal{R}(\eta)$  is the largest for  $0.2 < \eta < 1$  and it decays with  $\eta$  for  $\eta > 1$  (since both  $\Delta^{\text{inp}}$  and  $\varphi^{\text{inp}}$  decay with  $\eta$  for  $\eta > 1$ ).  $\mathcal{R}(\eta)$  is the largest when  $\gamma = 60^\circ$ . For the 1-storey building it reaches about 2.5, for the 10-storey building it reaches 5, and for the 50-storey building it is almost equal to 12. On the other end, for  $\gamma = 0^\circ$  and  $30^\circ$ , for the 1-storey building,  $\mathcal{R}(\eta) < 1$ ; then the additional rocking affects little the relative response and the fact that  $\Delta^{\text{inp}} < \Delta_{\text{com}}^{\text{inp}}$  prevails. For the 10-storey building, for  $\gamma = 0^\circ$ ,  $\mathcal{R}(\eta) \leq 1$  for all  $\eta$ 's; for  $\gamma = 30^\circ$ ,  $\mathcal{R}(\eta) > 1$  only for  $0.5 < \eta < 1.5$ , that is for frequencies higher than the frequency of the first mode of vibration ( $0.02 < \eta_N < 0.4$  for  $50 \text{ m/s} < \beta < 1000 \text{ m/s}$ ). For the 50-storey building, for  $\gamma = 0^\circ$  and  $30^\circ$ ,  $\mathcal{R}(\eta) < 1.8$  for all  $\eta$ 's, and for  $\eta < 0.12$  (where the peak response may be) it is practically equal to 1. Recalling the values of  $\eta_N$  for the three buildings and for  $50 \text{ m/s} < \beta < 1000 \text{ m/s}$ , and that the system frequency  $\eta^{\text{sys}} < \eta_N$ , it can be concluded that for  $\gamma = 0^\circ$  and  $30^\circ$  the peak response of the oscillator may not be underestimated by approximating  $\Delta^{\text{inp}}$  by  $\Delta_{\text{com}}^{\text{inp}}$ . For  $\gamma = 60^\circ$ , the peak response can be amplified (relative to excitation by  $\Delta_{\text{com}}^{\text{inp}}$ ) by a factor as large as 2.5 for the 1-storey building, by a factor up to 5 for the 10-storey building, and by one order of magnitude for the 50-storey building.

### Incident P-waves

Following a similar analysis as for incident SV-waves, from the curves in Fig. 6, the following can be concluded. The amplification  $\mathcal{R}(\eta)$  is the largest for  $\gamma = 30^\circ$ , that is when  $\varphi^{\text{inp}}$  is the largest. Because of the slow growth of  $\varphi^{\text{inp}}$  with  $\eta$  ( $\varphi^{\text{inp}}$  is larger only for  $\eta \geq 0.6$ ),  $\mathcal{R}(\eta) \leq 1$  for  $\eta < 0.6$  for the 1-storey building, for all the incident angles; for the 10-storey building  $\mathcal{R}(\eta)$  is also smaller for  $\eta < 0.6$  ( $\mathcal{R}(\eta) < 1.8$ ). The amplification is the largest for higher  $\eta$ 's. The largest value of  $\mathcal{R}(\eta)$  in the interval  $\eta \in (0, 2)$  is about 2 for the 1-storey building, about 3 for the 10-storey building, and about 3.5 for the 50-storey building. The peak response (at the system frequency) can be amplified by a factor of about 2 for the 1-storey building, 1.5 for the 10-storey building, and by a factor of almost 2 for the 50-storey building.

### Incident Rayleigh-waves

The amplification  $\mathcal{R}(\eta)$  has similar shape as  $\varphi^{\text{inp}}(\eta)$ . This can be seen from Fig. 4 and Fig. 7. It has local maxima near  $\eta = 0.5$  and  $1.5$  and local minima near  $\eta = 1$  and  $2$ .  $\varphi^{\text{inp}}$  for Rayleigh-waves is considerably larger relative to  $\varphi^{\text{inp}}$  for incident P-waves and incident SV-waves below critical angle, and it is comparable with  $\varphi^{\text{inp}}$  for incident SV-waves beyond critical angle. The maximum amplification is near  $\eta \approx 0.5$ . The maximum

value of  $\mathcal{R}(\eta)$  is less than 3.5 for the 1-storey building, about 5 for the 10-storey building, and about 9 for the 50-storey building. Recalling the intervals for  $\eta_N$ , for the examples considered here, the peak response may be amplified by a factor of about 3.5 for the 1-storey building, 4.5 for the 10-storey building, and by a factor of about 5.5 for the 50-storey building.

### $\mathcal{R}(\eta)$ for Shallow Foundations

For the three buildings in Figs. 5 and 6, but founded on «shallow» foundations ( $h/a = 0.5$ ),  $\mathcal{R}(\eta)$  is shown for incident P-waves ( $\gamma = 30^\circ, 60^\circ$  and  $85^\circ$ ) in Fig. 8, and for incident SV-waves ( $\gamma = 0^\circ$  and  $30^\circ$ ) in Fig. 9. In both figures  $m_i/m_s = 0.2$ , and the ratios  $m_b/m_f$  are chosen so that  $m_b$  is approximately the same as for the deeper foundations in Fig. 5 and Fig. 6.  $m_b/m_f = 2.4$  for the 1-storey building, 12 for the 10-storey building, and 40 for the 50-storey building.

For incident P-waves, for smaller  $\eta$ ,  $\mathcal{R}(\eta)$  has similar amplitudes both for  $h/a = 1$  and for  $h/a = 0.5$ . For higher  $\eta$ 's,  $\mathcal{R}(\eta)$  is larger for the buildings on shallow foundations, because of the larger amplitudes of  $\varphi^{\text{inp}}$ . For the examples presented here, for the 1-storey building, the maximum value of  $\mathcal{R}(\eta)$  in  $\eta \in (0, 2)$  is about 3, for the 10-storey building it is about 7 and for the 50-storey building it is about 17.

For incident SV-waves ( $\gamma = 0^\circ$  and  $30^\circ$ ), for the 1-storey building,  $\mathcal{R}(\eta) < 1$  (same as for the building on semi-circular foundation), and for the 10-storey building it is slightly larger than 1. For the 50-storey building, for small  $\eta$ 's,  $\mathcal{R}(\eta)$  is larger when the foundation is deeper, but for higher  $\eta$ 's it is larger when the foundation is shallow and it reaches the value 3.5 at  $\eta \approx 2$  ( $\gamma = 0^\circ$ ).

It can be concluded that for incident P-waves and incident SV-waves below critical angle (in both cases the free-field motion consists of body waves only), for very low  $\eta$ 's,  $\mathcal{R}(\eta)$  is the same or may be larger when the foundation is deeper. For higher  $\eta$ ,  $\mathcal{R}(\eta)$  is larger for shallow foundations ( $h/a = 0.5$ ).

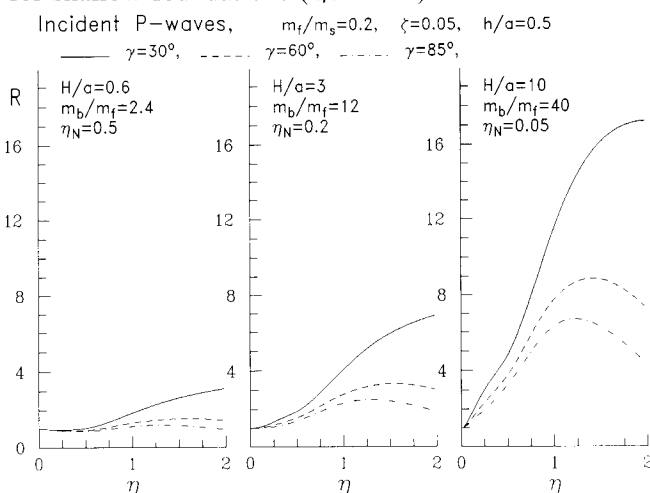


Fig. 8 –  $R = \mathcal{R}$  (the ratio of the relative response to the «true» foundation input motion  $\Delta^{\text{inp}}$ , and to the «common» approximation  $\Delta_{\text{com}}^{\text{inp}}$ ), versus the dimensionless frequency  $\eta$ , for incident plane P-waves, for three buildings (a 1-storey, a 10-storey, and a 50-storey) on shallow foundations ( $h/a = 0.5$ ). The different lines correspond to different incident angles.

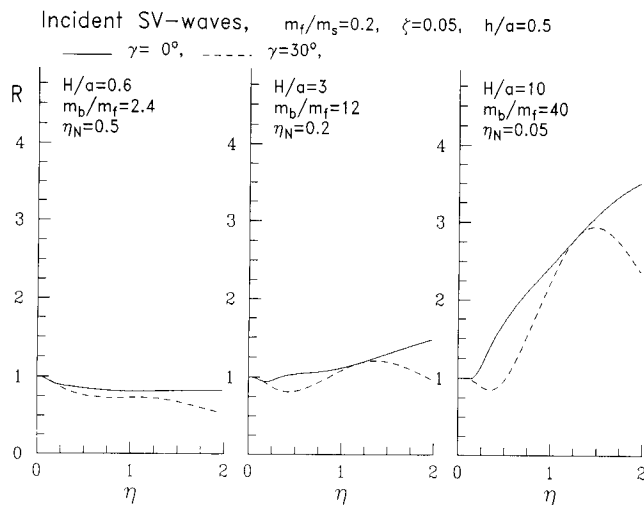


Fig. 9 –  $R \equiv \mathcal{R}$  (the ratio of the relative response to the «true» foundation input motion  $\Delta^{\text{inp}}$  and to the «common» approximation  $\Delta^{\text{inp}}_{\text{com}}$ ), versus the dimensionless frequency  $\eta$ , for incident plane SV-waves, for three buildings (a 1-storey, a 10-storey, and a 50-storey) on shallow foundations ( $h/a = 0.5$ ). The different lines correspond to different incident angles.

#### Effect of the building mass and of the foundation, mass on $\mathcal{R}(\eta)$

$\mathcal{R}(\eta)$  was calculated also for  $m_b/m_f$  twice larger and half of the typical values (see the section entitled Example Buildings in this paper). The results show that  $\mathcal{R}(\eta)$  varies little with  $m_b/m_f$  for the 1-storey building and not much for the 10-storey building. For smaller  $\eta$ 's,  $\mathcal{R}(\eta)$  appears to be slightly larger when the building is «lighter», and for larger  $\eta$ 's, when the building is «heavier». For the 50-storey building,  $\mathcal{R}(\eta)$  appears to be larger for all  $\eta$ 's (in the interval (0.2)) when the building is lighter. Those trends have been illustrated in Fig. 7, for incident Rayleigh-waves.

$\mathcal{R}(\eta)$  also depends on the foundation mass, with most obvious trends and most significantly for the 50-storey building. In Fig. 10,  $\mathcal{R}(\eta)$  is shown for the 50-storey building for  $m_f/m_s = 0.01, 0.2$  and  $0.4$ . The plot on the left-hand-side is for semi-circular foundations ( $h/a = 1$ ) and on the right-hand-side for shallow foundations ( $h/a = 0.5$ ). The excitation is a plane P-wave ( $\gamma = 30^\circ$ ). The building damping ratio,  $\zeta$ , and fixed-base frequency,  $\eta_N$ , have the same values as in Figs. 5 through 9; the ratio  $m_b/m_f$  is such that the building mass is equal to the typical value for the 50-storey building. It can be seen from this figure that, for the highest building,  $\mathcal{R}(\eta)$  is larger when the foundation is lighter.

Apparently, for the highest building (for which the interaction effects are more pronounced),  $\mathcal{R}(\eta)$  is smaller when the building and/or the foundation are «heavier». This may be because of the larger compliance forces (associated with heavier buildings) that reduce the relative response. It seems that larger input motion (the one that includes  $\varphi^{\text{inp}}$ ) is associated with larger reduction of the relative response (for heavier buildings and foundations).

Incident P-waves,  $\gamma = 30^\circ$ ,  $H/a = 10$ ,  $\zeta = 0.05$ ,  $\eta_N = 0.05$

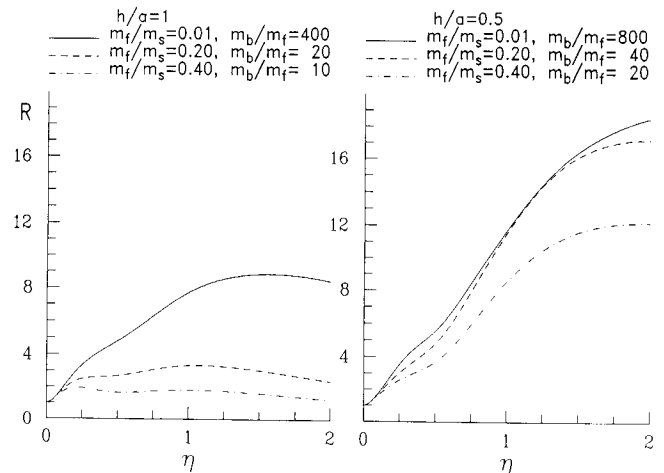


Fig. 10  $R \equiv \mathcal{R}$  (the ratio of the relative response to the «true» foundation input motion  $\Delta^{\text{inp}}$  and to the «common» approximation  $\Delta^{\text{inp}}_{\text{com}}$ ), versus the dimensionless frequency  $\eta$ , for incident plane P-waves ( $\gamma = 30^\circ$ ), for buildings on semicircular ( $h/a = 1$ ) and on shallow foundations ( $h/a = 0.5$ ). The different lines correspond to different values of the mass of the foundation. The mass of the building is the same for all the curves.

#### Summary and conclusions

The aim of this paper has been to estimate by how much the lateral relative displacements, and the associated internal forces, during transverse vibration of long buildings on flexible soil may be underestimated by neglecting the input rocking excitation of the building foundation (by approximating the foundation input motion in soil-structure interaction problems by a frequency independent translation only). For this purpose the ratio  $\mathcal{R}(\eta) = |u_b^{\text{rel}}|/|u_{b,\text{com}}^{\text{rel}}|$  has been defined, where  $u_b^{\text{rel}}$  is the response at frequency  $\eta$  to the «true» foundation input motion, and  $u_{b,\text{com}}^{\text{rel}}$  is the response to the «common» approximation of the foundation input motion.

Instrument recordings of the rocking component of strong ground motions are not available so far. Different authors use different analytical and numerical methods to estimate the amplitude and phase (relative to the translations) of the rocking component of ground motion. In this paper the building-soil model is two-dimensional (an equivalent single degree-of-freedom oscillator on a circular foundation embedded into a homogeneous and elastic half-space), and the excitations are plane P- and SV-waves and surface Rayleigh waves. In the real world, the geology between the earthquake source and the building site is much more complicated than a homogeneous elastic half-space, and is often not known in detail. The earthquake excitation is also more complicated than plane body waves and simple Rayleigh waves. However, our aim has not been to present a precise quantitative estimate for realistic three-dimensional case, but to consider a qualitative study, to see how different parameters of the soil-building system may affect the amplification  $\mathcal{R}(\eta)$ .

A 1-storey, a 10-storey and a 50-storey «buildings»



**Table 1** – Properties of shear-beam and equivalent single degree-of-freedom oscillator models for buildings with  $n = 1, 10$  and  $50$  stories

$n$	$T_N$	$H_{sb}$	$W_{sb}$	$\frac{H^*}{a}$	$\frac{r_b^*}{a}$	$\frac{m_b^{**}}{m_f}$	$\frac{m_f}{m_s}$	$\eta_{N,1}$	$\eta_{N,2}$
	(sec)	(m)	(m)					( $\beta = 1000$ m/s)	( $\beta = 50$ m/s)
1	0.1	5	10	0.58	0.58	1.27	0.2	0.1	2
10	1	50	20	2.9	0.58	6.36	0.2	0.02	0.4
50	5	250	30	9.36	0.58	21.2	0.2	0.006	0.12

\* it is assumed that  $W_{sb} = 2a$

\*\* the assigned values are for  $\rho_f/\rho_s = \rho_f/\rho_s = 0.2$  and for a semi-circular foundation.

were analyzed, supported by semicircular foundations and by «shallow» foundations ( $h/a = 0.5$ ). The results showed that  $\mathcal{R}(\eta)$  is mostly affected by the amplitude of the rocking component of the foundation input motion,  $\varphi^{inp}$ , and by the building height.  $\mathcal{R}(\eta)$  is larger when the input rotation is larger and when the building is higher. Of all the excitations considered, the foundation input rotation is the largest for incident SV-waves beyond critical angle and for incident Rayleigh waves. Throughout the spectrum  $\eta \in (0,2)$ , for buildings on semi-circular foundations, for incident SV-waves ( $\gamma = 60^\circ$ ),  $\mathcal{R}(\eta)$  can be as large as 2.5 for the 1-storey buildings, 5.5 for the 10-storey building and 12 for the 50-storey building. For incident P-waves (semi-circular foundation),  $\mathcal{R}(\eta)$  can be as large as 2 for the 1-storey building, 3 for the 10 storey building and 3.5 for the 50-storey building. For incident Rayleigh waves, it can be as large as 3 for the 1-storey building, 5 for the 10-storey building, and 9 for the 50-storey building. For the 1-storey building and for incident SV-waves below critical angle ( $\gamma = 0^\circ$  and  $30^\circ$ ),  $\mathcal{R}(\eta) \leq 1$  ( $\Delta_{com}^{inp} > \Delta_{com}^{inp} \neq 0$ ). As  $\eta \rightarrow 0$ ,  $\mathcal{R}(\eta) \rightarrow 1$ .

For incident P-waves and SV-waves below critical angle (when the free-field motion consists only of body waves), if the foundation is shallow ( $h/a = 0.5$ ), for low  $\eta$ 's,  $\mathcal{R}(\eta)$  may be slightly smaller as compared with  $\mathcal{R}(\eta)$  for the same buildings on deeper (semicircular) foundations. However, for higher  $\eta$ 's,  $\mathcal{R}(\eta)$  is larger when the foundation is shallow, because of the larger amplitudes of  $\varphi^{inp}$ .

The building and the foundation masses affect  $\mathcal{R}(\eta)$  through the compliance forces which modify the displacement at the building base. The effect of the mass is very small for the 1-storey building. The trend is most clear and the magnitude of this effect is the largest for the 50-storey building. For this building,  $\mathcal{R}(\eta)$  is smaller when the building and the foundation masses are larger. This is probably because of the larger compliance forces of the building (when it is «heavier») that reduce the relative building response and the effect of the additional rotational excitation.

## References

- /1/ Bielak, J. (1971). «Dynamics of Building Soil Interaction» Ph.D. Thesis, Calif. Inst. of Technology, Pasadena, California.
- /2/ Castellani, A. and G. Boffi (1986). «Rotational Components of the Surface Ground Motion During an Earthquake» *Earthquake Eng. and Structural Dynamics*, 14(5), 751-767.
- /3/ Castellani, A. and G. Boffi (1989). «On the Rotational Components of Seismic Motion» *Earthquake Eng. and Structural Dynamics*, 18(6), 785-797.
- /4/ Gupta, V.K. and M.D. Trifunac (1989). «Investigation of Building Response to Translational and Rotational Earthquake Excitations», Dept. of Civil Eng. Rep. No. 89-02, Univ. of Southern California, Los Angeles, California.
- /5/ Gupta, I.D. and M.D. Trifunac (1990a). «Probabilistic Spectrum Superposition for Response Analysis Including the Effects of Soil-Structure Interaction» *J. Probabilistic Engr. Mechanics*, 5(1), 9-18.
- /6/ Gupta, V.K. and M.D. Trifunac (1990b). «Response of Multistoried Buildings to Ground Translation and Rocking During Earthquakes» *J. Probabilistic Engr. Mechanics*, 5(3), 138-145.
- /7/ Gupta, V.K. and M.D. Trifunac (1991). «Effects of Ground Rocking on Dynamic Response of Multistoried Buildings During Earthquakes», *Structural Eng./Earthquake Eng.*, JSCE, 8(2), 43-50.
- /8/ Lee, V.W. and M.D. Trifunac (1985). «Torsional Accelerograms» *Soil Dynamics and Earthquake Engineering*, 4(3), 132-139.
- /9/ Lee, V.W. and M.D. Trifunac (1987). «Rocking Strong Earthquake Accelerations» *Soil Dynamics and Earthquake Engineering*, 6(2), 75-89.
- /10/ Luco, J.E. (1980). «Seismic Safety Margins Research Program (Phase I), Linear Soil Structure Interaction» Report to Nuclear Testing Eng. Division, Lawrence Livermore Lab., Livermore, California.
- /11/ Lomnitz, C. (1990). «Mexico 1985: the Case for Gravity Waves» *Geophys. J. Int.*, 102, 569-572.
- /12/ Niazi, M. (1986). «Inferred Displacements, Velocities and Rotations of a Long Rigid Foundation Located at El Centro Differential Array Site During the 1979 Imperial Valley, California, Earthquake» *Earthquake Engineering and Structural Dynamics*, 14(4), 531-542.
- /13/ Todorovska, M.I. (1992). «Effects of the Depth of the Embedment on the System Response During Building Soil Interaction» *Soil Dynamics and Earthquake Engineering*, (in press).
- /14/ Todorovska, M.I. and M.D. Trifunac (1990). «Analytical Model for in-plane Building Foundation-

Soil Interaction: Incident P-, SV- and Rayleigh Waves» Dept of Civil Engr. Report No. CE 90-01, Univ. of Southern California, Los Angeles, California.

- /15/ Todorovska, M.I. and M.D. Trifunac (1992). «The System Damping, the System Frequency and the System Response Amplitudes During In-Plane Building-Soil Interaction» Earthquake Eng. and Struct. Dynamics, 21(2), 127-144.
- /16/ Trifunac, M.D. (1971). «Response Envelope Spectrum and Interpretation of Strong Earthquake

Ground Motion» Bull. Seism. Soc. America, 61, 343-356.

- /17/ Trifunac, M.D. (1972). «Tectonic Stress and Source Mechanism of the Imperial Valley, California Earthquake of 1940» Bull. Seism. Soc. America, 62, 1283-1302.
- /18/ Trifunac, M.D. (1982). «A Note on Rotational Components of Earthquake Motions on Ground Surface for Incident Body Waves» Soil Dynamics and Earthquake Eng., 1(1), 11-19.

## Appendix A: list of symbols

- $\beta, \mu, \nu$  = shear wave velocity, shear modulus, and Poisson's ratio for the soil
- $h, a$  = depth and half-width of the foundation
- $\omega, T$  = circular frequency and period of the incident wave
- $\eta = \frac{\omega a}{\pi \beta} = \frac{2a}{\beta T}$  = dimensionless frequency
- $H_{sb}, W_{sb}$  = height and width of a shear-beam building model
- $H, r_b = \frac{W_{sb}}{\sqrt{12}}$  = height and radius of gyration of the equivalent SDOF building model
- $\zeta, \omega_N$  = viscous damping ratio and fixed-base natural frequency of the equivalent SDOF building model
- $\eta_N = \frac{\omega_N a}{\pi \beta}$  = dimensionless stiffness parameter of the building relative to the soil
- $\eta^{sys}$  = dimensionless system frequency
- $g$  = acceleration due to gravity
- $\Delta, V, \varphi$  = horizontal and vertical displacements and rocking angle of point O on the foundation
- $\psi^{rel}, u_b^{rel}$  = relative angle of rocking, and relative horizontal displacements of the equivalent SDOF building model
- $\Delta = \{V, \Delta, \varphi a\}^T$  = generalized displacement vector describing the motion of point O
- $\Delta^{inp} = \{V^{inp}, \Delta^{inp}, \varphi^{inp} a\}^T$  = generalized displacement vector of the foundation input motion (response of a massless foundation to the incident waves)
- $\Delta_{com}^{inp} = \{0, u^{ff}, 0\}^T$  = generalized displacement vector of the commonly used approximation for the foundation input motion
- $u^{ff}$  = horizontal component of the free-field motion at  $z = 0$
- $u_{b,com}^{rel}$  = relative building response when the foundation input motion is described by generalized vector  $\Delta_{com}^{inp}$
- $\mathcal{R}(\eta) = |u_b^{rel}| / |u_{b,com}^{rel}|$  = ratio of the relative response to the «true» foundation input motion  $\Delta^{inp}$  and to the «common» approximation  $\Delta_{com}^{inp}$
- $\gamma$  = incident angle of the plane P- and SV-waves, measured from the normal to the half-space surface.

## Appendix B

Let  $\mathbf{F}^{(b)} = \{f_z^{(b)}, f_x^{(b)}, M_0^{(b)} / H\}^T$  be a generalized force vector of the forces that the foundation exerts onto the building. The vertical force  $f_z^{(s)}$  (up), the horizontal force  $f_x^{(b)}$  (in the negative  $x$ -direction) and the moment about O,  $M_0^{(b)}$  (counter-clockwise), see Fig. 1, can be calculated, given the displacement of the foundation, as follows

$$\mathbf{F}^{(b)} = m_b \omega^2 \left[ [K^{(b)}] + [C_g^{(b)}] \right] \Delta_0 e^{-i\omega t} \quad (B1)$$

where

$$[C_g^{(b)}] = \frac{g}{\omega^2 H} \begin{bmatrix} 0 & 0 & 0 \\ 0 & 0 & c_{23} \\ 0 & c_{32} & c_{33} \end{bmatrix} \quad (B2)$$

is the complex stiffness matrix for the building, and

$$[K_g^{(b)}] = \frac{g}{\omega^2 H} \begin{bmatrix} 0 & 0 & 0 \\ 0 & 0 & c_{23} \\ 0 & c_{23} & c_{33} \end{bmatrix} \quad (B3)$$

The entries of  $[K^{(b)}]$  and  $[C_g^{(b)}]$  are

$$k_{11} = 1 \quad (B4a)$$

$$k_{22} = 1 + \frac{m_b H^2}{I_0} \left( \frac{\omega}{\omega_N} \right)^2 \frac{1}{q} \quad (B4b)$$

$$k_{23} = 1 + \left( \frac{\omega}{\omega_N} \right)^2 \frac{1}{q} \quad (B4c)$$

$$k_{32} = k_{23} \quad (B4d)$$

$$k_{33} = \frac{I_0}{m_b H^2} \left[ 1 + \left( \frac{\omega}{\omega_N} \right)^2 \frac{1}{q} \right], \quad (\text{B4e})$$

where

$$q = 1 - 2i\zeta \frac{\omega}{\omega_N} - \left( \frac{\omega}{\omega_N} \right)^2 - \frac{g}{\omega^2 H} \left( \frac{\omega}{\omega_N} \right)^2 \frac{m_b H^2}{I_0} \quad (\text{B4f})$$

and

$$c_{23} = \frac{m_b H^2}{I_0} \left( \frac{\omega}{\omega_N} \right)^2 \frac{1}{q} \quad (\text{B5a})$$

$$c_{32} = c_{23} \quad (\text{B5b})$$

$$c_{33} = 1 + 2 \left( \frac{\omega}{\omega_N} \right)^2 \frac{1}{q} + \frac{m_b H^2}{I_0} \left( \frac{\omega}{\omega_N} \right)^2 \frac{1}{q} \frac{g}{\omega^2 H}. \quad (\text{B5c})$$